The impact of greenhouse gases on past changes in tropospheric ozone

C. Lang,[1] D. W. Waugh,[1] M. A. Olsen,[2,3] A. R. Douglass,[3] Q. Liang,[3,4] J. E. Nielsen,[3,5] L. D. Oman,[3] S. Pawson,[3] and R. S. Stolarski[1,3]

Received 14 June 2012; revised 22 October 2012; accepted 23 October 2012; published 13 December 2012.

[1] The impact of changes in the abundance of greenhouse gases (GHGs) on the evolution of tropospheric ozone (O_3) between 1960 and 2005 is examined using a version of the Goddard Earth Observing System chemistry-climate model (GEOS CCM) with a combined troposphere-stratosphere chemical mechanism. Simulations are performed to isolate the relative role of increases in methane (CH_4) and stratospheric ozone depleting substances (ODSs) on tropospheric O_3. The 1960 to 2005 increases in GHGs (CO_2, N_2O, CH_4, and ODSs) cause increases of around 1–8% in zonal-mean tropospheric O_3 in the tropics and northern extratropics, but decreases of 2–4% in most of the southern extratropics. These O_3 changes are due primarily to increases in CH_4 and ODSs, which cause changes of comparable magnitude but opposite sign. The CH_4-related increases in O_3 are similar in each hemisphere (~6%), but the ODS-related decreases in the southern extratropics are much larger than in northern extratropics (10% compared to 2%). This results in an interhemispheric difference in the sign of past O_3 change. Increases in the other GHGs (CO_2 and N_2O) and SSTs have only a small impact on the total burden over this period, but do cause zonal variations in the sign of changes in tropical O_3 that are coupled to changes in vertical velocities and water vapor.

Citation: Lang, C., D. W. Waugh, M. A. Olsen, A. R. Douglass, Q. Liang, J. E. Nielsen, L. D. Oman, S. Pawson, and R. S. Stolarski (2012), The impact of greenhouse gases on past changes in tropospheric ozone, *J. Geophys. Res.*, *117*, D23304, doi:10.1029/2012JD018293.

1. Introduction

[2] Understanding the distribution and evolution of tropospheric ozone (O_3) is important for several different reasons. First, O_3 absorbs infrared radiation and in terms of radiative forcing over the last 150 years is the third most important greenhouse gas (GHG) behind carbon dioxide (CO_2) and methane (CH_4) [*Intergovernmental Panel on Climate Change*, 2007]. Second, O_3 causes respiratory system problems and thus it is a major concern for air quality [*World Health Organizaton*, 2006]. Third, O_3 is the primary source of the hydroxyl radical (OH) and plays a key role in tropospheric chemistry and the fate of tropospheric pollutants.

[3] Tropospheric O_3 has increased significantly since pre-industrial times due to increases in surface emissions of O_3 precursor gases such as carbon monoxide (CO), hydrocarbons, and nitrogen oxides (NO_x) [*Shindell et al.*, 2006; *Wang and Jacob*, 1998]. However, other factors also influence past changes in O_3. Increases in greenhouse gases (GHGs) have the potential to alter tropospheric O_3 by increasing the temperature and humidity, and previous modeling studies have shown a net decrease in tropospheric O_3 burden in a warmer, wetter climate [*Zeng et al.*, 2008]. Increases in GHGs can also impact tropospheric O_3 through changes in the transport within the troposphere and between the stratosphere and troposphere [*Liang et al.*, 2009; *Shindell et al.*, 2006]. Several GHGs also influence tropospheric O_3 by other mechanisms. CH_4 is an O_3 precursor gas, and an increase in CH_4 leads to an increase in tropospheric O_3 burden from increased in situ production [*Fiore et al.*, 2002, 2008]. Chlorofluorocarbons (CFCs) and other halogens, which are collectively known as ozone-depleting substances (ODSs), are source gases for chlorine and bromine radicals that deplete stratospheric O_3. This stratospheric O_3 depletion alters tropospheric O_3 by decreasing the flux of O_3 into the troposphere and increasing UV penetration into the troposphere [*Fuglestvedt et al.*, 1994;

[1]Department of Earth and Planetary Sciences, Johns Hopkins University, Baltimore, Maryland, USA.
[2]Goddard Earth Sciences Technology and Research, Morgan State University, Baltimore, Maryland, USA.
[3]NASA Goddard Space Flight Center, Greenbelt, Maryland, USA.
[4]Goddard Earth Sciences Technology and Research, Universities Research Space Association, Columbia, Maryland, USA.
[5]Science Systems and Application Incorporated, Lanham, Maryland, USA.

Corresponding author: D. W. Waugh, Department of Earth and Planetary Sciences, Johns Hopkins University, 3400 N. Charles St., Baltimore, MD 21218, USA. (waugh@jhu.edu)

©2012. American Geophysical Union. All Rights Reserved.
0148-0227/12/2012JD018293

Table 1. Summary of GEOS CCM Simulations: Years Used for SSTs/SICs and Surface Mean Mixing Ratios of GHGs[a]

Name	SSTs/SICs	CO_2 (ppm)	N_2O (ppb)	CH_4 (ppb)	Cl_{tot} (ppb)
TS1960	1950–1969	316	291	1270	0.82
TS2005	1985–2004	378	320	1810	3.35
TS2005-ODS	1985–2004	378	320	1810	0.83
TS2005-CH_4	1985–2004	378	320	1270	3.35

[a]The mixing ratio of both chlorine and bromine containing ODSs were varied among simulation, but only the total chlorine (Cl_{tot}) is listed. In all simulations the precursor emissions and aerosols are prescribed at 2005 levels.

Lelieveld and Dentener, 2000; *Shindell et al.*, 2006; *Thompson*, 1991].

[4] Numerous modeling studies have examined how GHGs impact tropospheric O_3 by changing climate or stratospheric O_3 [*Fiore et al.*, 2008; *Gauss et al.*, 2006; *Lelieveld and Dentener*, 2000; *Shindell et al.*, 2006; *Stevenson et al.*, 2006; *Sudo et al.*, 2003; *Wu et al.*, 2008; *Zeng et al.*, 2008, 2010]. However, the models used in these studies generally do not include all processes or couplings that can impact tropospheric O_3, e.g., the models have prescribed stratospheric O_3 or simplified stratosphere chemistry schemes, or use prescribed meteorological fields with no feedbacks between changes in composition and dynamics. Furthermore, most studies have focused on interannual variability or future trends, and few have examined the impact of past increases of GHGs on tropospheric O_3. Exceptions include the studies of *Gauss et al.* [2006], *Lamarque et al.* [2010] and *Shindell et al.* [2006] which examined the evolution of tropospheric O_3 from pre-industrial to present-day in simulations of chemistry-climate models with increasing GHGs (including ODSs) and precursor emissions. *Gauss et al.* [2006], separated the impact of GHGs and ODSs from that of precursor emissions, while *Shindell et al.* [2009] separated the impact of GHGs but not the impact of ODSs. *Lamarque and Solomon* [2010] performed chemistry-climate model simulations of the impact of climate change and ODSs on ozone from 1979 to 2005, including simulations to separate the different factors. However, the focus of their analysis was on stratospheric ozone.

[5] In this study we examine the impact of changes in GHGs between 1960 and 2005 on tropospheric O_3 using a stratosphere-resolving chemistry-climate model that has a combined troposphere-stratosphere chemical mechanism. In this model changes in GHGs impact tropospheric O_3 through changes in the dynamics, tropospheric chemistry, and stratospheric O_3. We examine not only the net effect of all GHGs on tropospheric O_3, but also the relative roles of increases of individual GHGs.

[6] In section 2 we describe the model used and simulations performed in this study. In section 3, we evaluate the simulated climatological distribution of O_3 by comparison with in situ and satellite observations. The simulated O_3 change between 1960 and 2005, and the role of different GHGs, is examined in section 4. Concluding remarks are in section 5.

2. Model Description and Simulations

2.1. Model Description

[7] The model used in this study is the Goddard Earth Observing System Chemistry Climate Model (GEOS CCM). The version of the model considered here couples version 5 of the GEOS general circulation model (GCM) [*Rienecker et al.*, 2008] with the comprehensive combined troposphere-stratosphere chemistry mechanism used in the Global Modeling Initiative (GMI) chemical transport model [*Duncan et al.*, 2007; *Strahan et al.*, 2007]. This troposphere-stratosphere chemistry mechanism has 117 species, 322 chemical reactions, and 81 photolysis reactions, and combines a detailed description of O_3-NO_x-hydrocarbon chemistry necessary for the troposphere [*Bey et al.*, 2001] with all important chemical reactions for the stratosphere [*Douglass et al.*, 2004], as described in *Duncan et al.* [2007].

[8] There has been extensive evaluation and use of earlier versions of GEOS CCM that included only stratospheric chemistry with tropospheric O_3 relaxing to a prescribed distribution [e.g., *Pawson et al.*, 2008]. The stratospheric chemistry version of GEOS CCM has been shown to perform well in simulating stratospheric dynamics and composition [e.g., *Eyring et al.*, 2010], and has been used in a range of studies on topics including the evolution of stratospheric O_3 and role of climate change [*Li et al.*, 2009; *Waugh et al.*, 2009], the cause of stratospheric temperature trends [*Stolarski et al.*, 2010], and what would have happened without regulations of CFCs [*Newman et al.*, 2009]. There has also been extensive evaluation of the GMI chemical transport model, including the tropospheric chemistry and composition in versions using meteorological fields from version 4 of GEOS GCM [*Considine et al.*, 2008; *Duncan et al.*, 2007; *Strahan et al.*, 2007; *Ziemke et al.*, 2006]. These have shown that the GMI model produces a realistic distribution of the tropospheric O_3 and CO, although tropospheric O_3 in simulations using the GCM meteorology has a high bias in northern middle latitudes.

2.2. Model Simulations

[9] The results presented in this study use the output from a series of GEOS CCM "time slice" simulations, in which the surface mixing ratios of the major long-lived GHGs (CO_2, CH_4, N_2O and CFCs), sea surface temperatures (SSTs), and sea ice concentrations (SICs) are prescribed as boundary conditions. The prescribed GHG mixing ratios are the observed monthly mean values for 1960 or 2005, while the SSTs and SICs cycle over observed values (*Rayner et al.* [2003], updated on a monthly basis) for 1950 to 1969 or 1985 to 2004; see Table 1. (The use of interannually varying SSTs allows the impact of this variability of composition to be examined. For example, *Oman et al.* [2011] show that GEOS CCM simulations using prescribed SSTs reproduce the observed response of tropospheric O_3 to ENSO.)

[10] In all simulations the monthly mean emissions of non-methane O_3 precursor gases (e.g., NO_x, CO, VOCs) and the monthly mean three-dimensional distribution of aerosols are also prescribed using values from the World Climate Research Programme (WCRP) Coupled Model Intercomparison Project 5 (CMIP5) (http://cmip-pcmdi.llnl.gov/cmip5/). In addition to the above fixed emissions, temperature-dependent parameterizations of isoprene from vegetation and NO from soil microbes, as described in *Duncan et al.* [2007], are included in all simulations. The monthly mean emissions of NO_x from lightning in all simulations are based on the climatology described in *Duncan et al.* [2007]. As the non-methane O_3 precursors and aerosols emissions are the same in all simulations, the differences in tropospheric O_3 between simulations are due to climate change caused by increases in GHGs,

Table 2. Definition of Difference Between Simulations

Name	Difference Between Simulations	Factors Changing
ΔPast	TS2005 − TS1960	All GHGs and SSTs
ΔODS	TS2005 − TS2005-ODS	ODS
ΔCH_4	TS2005 − TS2005-CH_4	CH_4
ΔCO_2	ΔPast − ΔODS − ΔCH_4	"CO_2 and SSTs"

ODS-induced stratospheric O_3 depletion, and changes in CH_4 concentrations. There is also a small contribution due to temperature-induced changes in the emissions of isoprene from vegetation and NO from soil microbes.

[11] To isolate the impact of the GHGs on tropospheric O_3 a series of time-slice integrations are performed that differed only in the prescribed surface values of GHGs. A pair of integrations is performed when all GHGs (CO_2, N_2O, CH_4, ODSs) and the SSTs are set at observed values for either 1960 or 2005. These simulations are referred as TS1960 and TS2005, respectively (see Table 1). Two additional simulations are performed that are the same as the TS2005 except that either the CH_4 or ODSs boundary conditions are specified at 1960 levels. These are referred to as TS2005-CH_4 and TS2005-ODS, respectively. (Note that although increases in N_2O and CH_4 can also contribute to stratospheric ozone loss we do not include them within ODSs, which are conventionally restricted to chlorine and bromine species. Also, the increases in N_2O and CH_4 from 1960 to 2005 have a small impact on stratospheric ozone.)

[12] In the analysis below we focus on the difference in O_3 and other fields between pairs of simulations, and use the following notation (Table 2): ΔODS refers to the difference between TS2005 and TS2005-ODS, and isolates the role of changes in ODSs. ΔCH_4 refers to the difference between TS2005 and TS2005-CH_4, and isolates the role of changes in CH_4. We estimate the combined impact of CO_2, N_2O and SSTs by calculating the "residual" between the 1960 and 2005 simulations, i.e., ΔPast − ΔODS − ΔCH_4 (or equivalently, TS2005-CH_4 + TS2005-ODS − TS2005 − TS1960). Although this term includes the impact N_2O and SSTs as well as any nonlinearity in the system, we refer for simplicity to this difference as ΔCO_2.

[13] All simulations started with 10 years of spin up and then ran for another 20 years. Monthly averages of chemical and meteorological fields were archived, and our analysis is based on these monthly averages from the last 20 years. Differences between simulations are presented as percentage change relative to the value for the TS2005 simulation. The statistical significance of differences between simulations is determined using the student-t test.

3. Model Evaluation

[14] As discussed in section 2, the model used here includes troposphere-stratosphere chemistry module from the GMI CTM within the GEOS CCM. Both the GEOS CCM with stratospheric chemistry and GMI CTM with combined troposphere-stratosphere chemistry have had extensive evaluation and are being used in a wide range of studies. There is, however, still a need to evaluate simulations from the GEOS CCM with troposphere-stratosphere chemistry coupled to radiation and dynamics. As the stratospheric O_3 in this version is similar to that from the well-evaluated stratospheric chemistry version of GEOS CCM, we focus here on the evaluation of the simulated tropospheric O_3 distribution.

[15] We first compare the TS2005 simulation with an update of the *Logan* [1999] ozonesonde climatology as described in *Considine et al.* [2008]. This climatology is formed by averaging the data in 35 layers equally spaced in pressure altitude between 1000 and 5 hPa (~1 km). The data set includes the climatological monthly mean O_3 mixing ratios, as well as the variance about this mean, for each station. For most stations the climatology is based on data for years 1990 to 2005. The location and time period of measurements for each station is given in the auxiliary material.[1]

[16] Comparison of vertical profiles for each station shows that the simulation captures the large-scale variations in tropospheric O_3, with weaker vertical gradients in the tropics than the extratropics, and larger tropospheric column values in northern than southern middle latitudes (see auxiliary material). In the SH and tropics there is quantitative agreement between the model and ozonesondes, but in NH mid and high latitudes there is a systematically high bias in the model. This can be seen in Figures 1a–1c, which show scatterplots of simulated versus ozonesonde annual-mean O_3 at 200, 500 and 750 hPa, respectively, for all 40 ozonesonde stations (different symbols are used for stations in different latitude bands). The high bias in the NH extends throughout the troposphere and increases from around 10% in the lower troposphere to 20%–40% in the lowermost stratosphere. This high bias in northern extratropical upper troposphere/lower stratosphere is similar to the bias in tropopause O_3 within the GMI CTM using GEOS GCM meteorology [*Considine et al.*, 2008].

[17] The surface distribution of O_3 in the model is evaluated by comparing with observations from the World Data Centre for Surface Ozone (WDCSO) (http://gaw.kishou.go.jp/wdcgg.html). The time period of the surface observations varies among the stations; see auxiliary material for list of stations and periods of available data. There is again generally good agreement between the climatological mean simulated and measured surface values but with a high bias in the NH mid and high latitudes; see Figure 1d.

[18] The above comparisons have considered only annual-mean O_3 but in many regions there are large seasonal variations in O_3. To evaluate the simulation of the seasonal cycle we compare the simulated and ozonesonde climatological seasonal cycles for several different latitude bands and altitudes; see Figure 2. (Note, the standard deviations shown in Figure 2 differ between the data and model: For the data it is the standard deviation of all daily values, whereas for the model it is based on monthly mean values.) Overall, the seasonal variation is well simulated by GEOS CCM, although the simulated amplitude tends to be less than observed in the middle troposphere and northern hemisphere lower troposphere, and the timing of the annual maximum in the SH lower stratosphere is later in the simulation than observed. Figure 2 also shows that model high bias in tropospheric O_3 in northern mid-high latitude is largest during winter. Similar seasonal variations are found if O_3 is averaged over midlatitudes (30–60N/S) or high latitudes (60–90N/S) separately. In particular, a similar high bias occurs for both northern midlatitudes and

[1]Auxiliary materials are available with the HTML. doi:10.1029/2012jd018293.

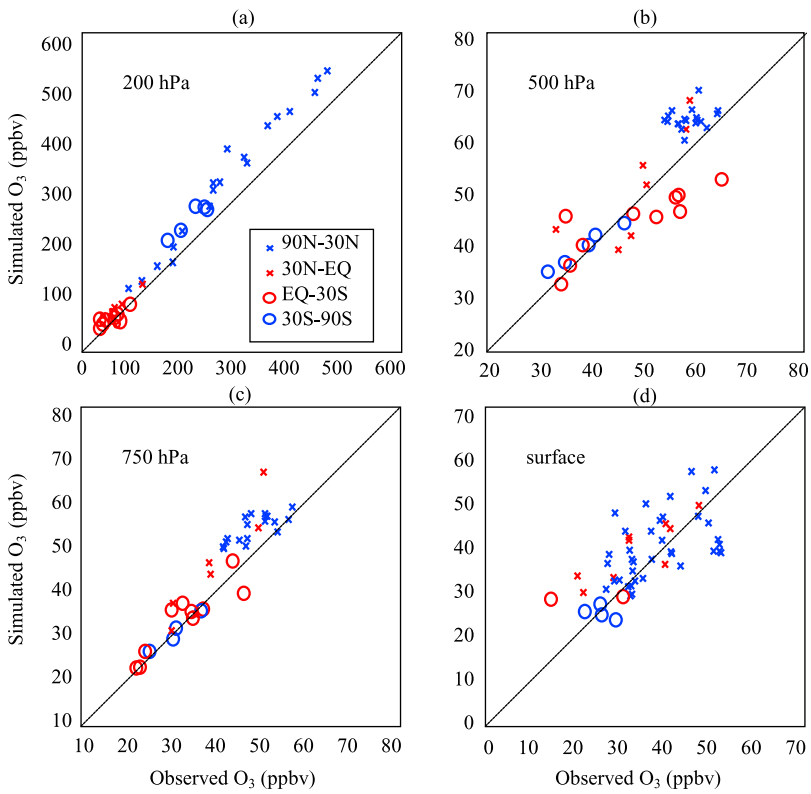

Figure 1. Comparison of simulated and observed annual-mean O_3 at (a) 200, (b) 500, (c) 750 hPa, and (d) the surface, for the TS2005 simulation. Observations in Figures 1a–1c are from ozonesonde, while in those in Figure 1d are from ground stations. Different symbols correspond to stations at different latitude bands (see Figure 1a).

northern high latitudes. Although Figures 1 and 2 show differences between the GEOS CCM simulation and observations, the differences are smaller than many of the models in the multimodel evaluation of *Stevenson et al.* [2006] (see their Figure 2, which shows ozone averaged over the same regions as in Figure 2 here for a suite of models).

[19] The ozonesonde and surface observations have limited spatial coverage and do not provide a global view of the O_3 distribution. We therefore consider measurements of the total tropospheric column O_3 (TCO) obtained from the Microwave Limb Sounder (MLS) and Ozone Monitoring Instrument (OMI) satellite instruments [*Ziemke et al.*, 2006]. The OMI/MLS TCO data cover the period 2005–2009, and provide coverage from 60°S to 60°N. The OMI/MLS TCO is calculated using the World Meteorological Organization (WMO) definition of the tropopause, whereas the model TCO is calculated using a "blended" tropopause that is in the standard output from the model. This blended tropopause is the lower of the height of a potential vorticity based tropopause and height of a thermally defined tropopause. Analysis of archived tropopause height from other (but similar) model simulations shows that the monthly mean blended tropopause pressure tends to be larger than the thermal tropopause in the extratropics (by around 10 hPa), and extratropical TCO defined using the blended tropopause is around 1.5 DU smaller than if the thermal tropopause is used.

[20] Figures 3a and 3b show the observed and simulated annual mean TCO, respectively. There is good agreement in the spatial variations of TCO, e.g., low values over tropical Pacific Ocean, high values over northern midlatitudes. However, consistent with the above comparison with ozonesondes, the model is around 20% higher over NH continents. This difference is much larger than difference expected from difference in the tropopause definition used to calculate the TCO (see above). As shown in Figures 3c and 3d, there is also good agreement in the seasonal variations of TCO, although (again consistent with the ozonesonde comparison) the simulated amplitude of the seasonal cycle is smaller than observed in the NH. The discrepancies between simulated and observed TCO shown in Figure 3 are again very similar to that for the GMI CTM simulation using GEOS GCM meteorology; see *Ziemke et al.* [2006].

[21] It is unclear what is causing the NH bias in the model. One possibility is a bias in the transport of stratospheric O_3 into the troposphere (which is an important process in determining the tropospheric O_3 distribution). To evaluate the simulated O_3 STE we use the simple mass balance approach first used to calculate mass STE by *Appenzeller et al.* [1996] and later used to calculate O_3 STE by *Olsen et al.* [2004] and *Hegglin and Shepherd* [2009]. In our calculation, following *Olsen et al.* [2004], the flux across the tropopause (F_{out}) is calculated by: $F_{out}(t) = dM/dt + F_{in}(t)$, where dM/dt is the mass change rate of the lowermost stratosphere and F_{in} is the net inflow from the overworld (the portion of stratosphere above 380 K isentropic surface) to lowermost stratosphere. For mass STE the change/inflow of air mass is used, whereas for O_3 STE the change/inflow of O_3 is used. This calculation yields an annual mean

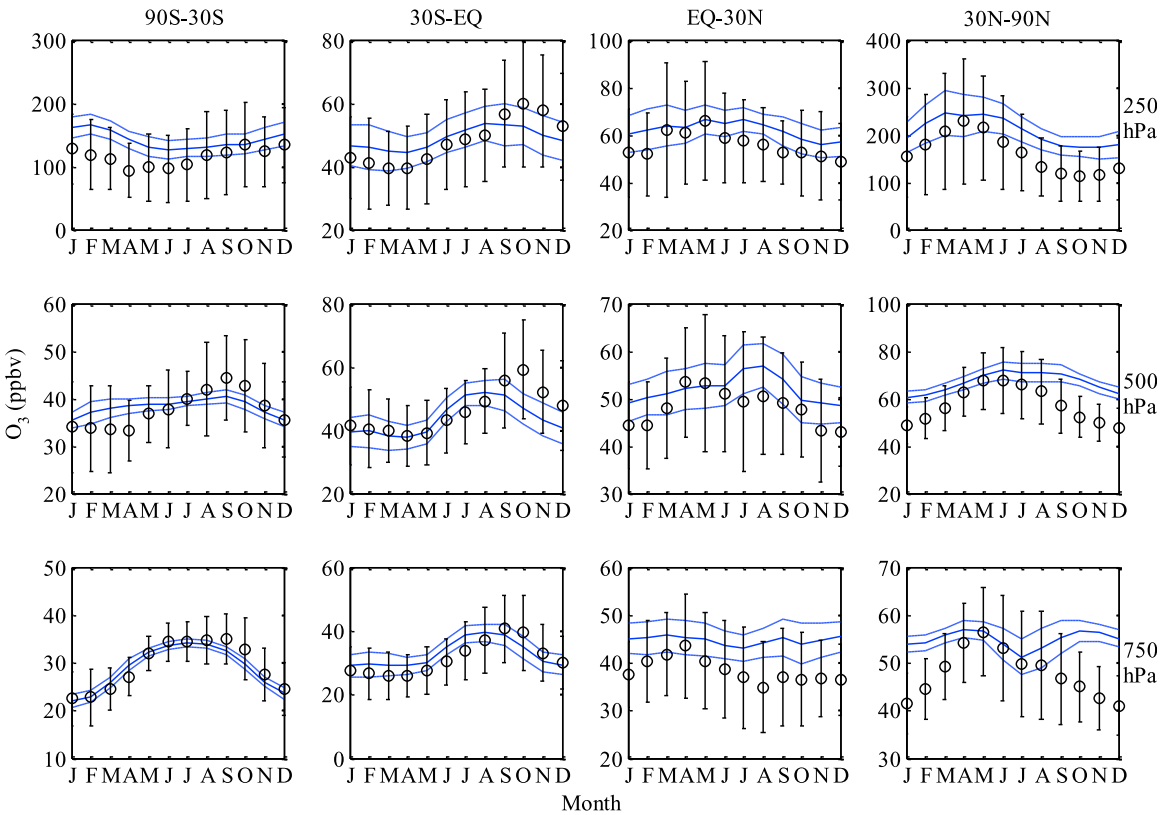

Figure 2. Comparison of simulated (curves) and observed (circles) climatological seasonal cycle of O_3, for four different latitude bands: (left to right) 90–30°S, 30–0°S, 0–30°N, and 30–90°N; and three pressure levels: (top to bottom) 250, 500, and 750 hPa. The vertical bars are the average of the daily standard deviations of observation for each station, while the outer curves show plus and minus one interannual standard deviation of the model.

O_3 STE for TS2005 simulation of 285 and 210 Tg/y for the NH and SH, respectively. These values are in good agreement with values of 275 and 214 Tg/y obtained from the same calculations using O_3 measurements from the MLS satellite instrument and meteorological fields from MERRA reanalysis for 2005 to 2010 [*Olsen et al.*, 2012]. There is also good agreement in the seasonal variation of the O_3 STE, with both model and observation based calculations showing spring maxima for both hemispheres. The good agreement in annual mean values and seasonal variations suggests that O_3 STE is not the cause of the high bias in NH tropospheric O_3. A similar conclusion was reached by *Considine et al.* [2008] in their analysis of the high bias in the GMI CTM.

[22] The above evaluation has focused only on the simulated O_3 distribution. The model performance has also been evaluated for CO, NO, and PAN. Comparison of surface CO with observation from the NOAA ESRL Carbon Cycle Cooperative Global Air Sampling Network [*Novelli and Masarie*, 2010] shows that the model captures the seasonal variations in extra-tropical stations, but the model underestimates the concentrations over the NH, by around 10–20 ppb (see auxiliary material). This model-data bias is again similar to that in the GMI CTM simulation discussed above [*Duncan et al.*, 2007].

[23] There is also generally good agreement of concentration and vertical structure of CO, NO and PAN between the simulation and aircraft measurements made during several NASA campaigns in the 1990s [*Emmons et al.*, 2000] (see auxiliary material). For example, the simulations produce a maximum in NO in the lower troposphere and the near constant vertical profiles of tropical CO. The model-data agreement is generally similar or better than that for the simulations shown in *Emmons et al.* [2000] and *Zeng et al.* [2008].

4. The 1960–2005 Changes

4.1. O_3 Changes

[24] We now examine the simulated change in O_3 between the 1960 and 2005 due to increases in GHGs. Figure 4a shows the percentage change in annual-mean zonal-mean O_3 between simulations, relative to TS2005 O_3. The crosses show regions where the differences between the simulations are not statistically significant at the 95% confidence level. The most striking result is that tropospheric O_3 decreases in the SH extra-tropics but increases in the tropics and NH. For most of the SH lower to middle troposphere the decrease is around 2%–4%, with larger decreases and a strong vertical gradient in the upper troposphere. The increases in tropospheric O_3 near the equator and in the NH are of similar magnitude to the SH decrease, except near the subtropical jets where increases are around 8%. In contrast to the troposphere, there is a decrease in stratospheric O_3 in both hemispheres. The decrease is much larger in the SH, where there is a ~60% decrease in

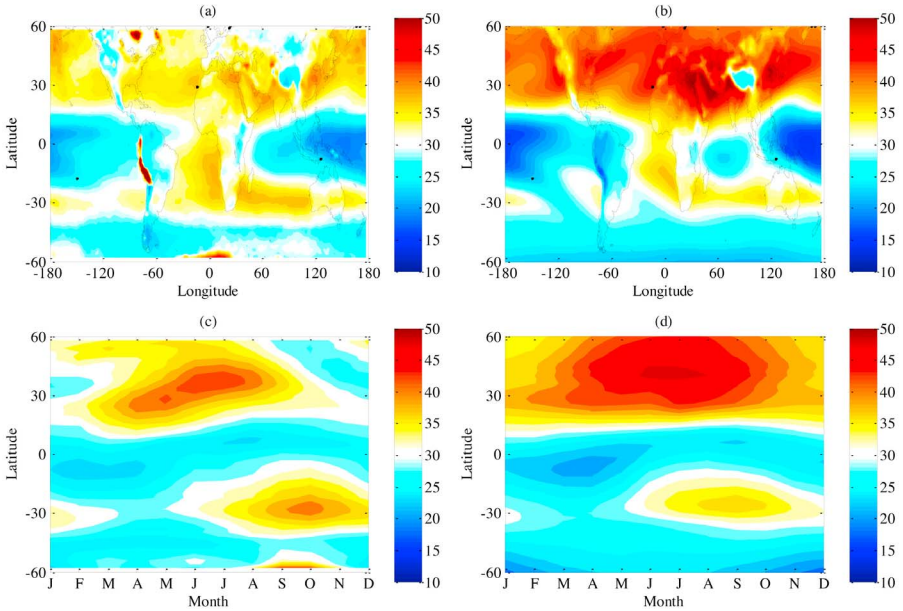

Figure 3. Annual-mean tropospheric column ozone (TCO), in DU, for (a) OMI/MLS measurements and (b) the TS2005 simulation, and climatological seasonal cycle of zonal-mean TCO for (c) OMI/MLS measurements and (d) the TS2005 simulation.

annual-mean Antarctic lower stratospheric O_3 from 1960 to 2005 (the color scale in Figure 4 saturates at ±20%).

[25] We are not aware of other studies examining the impact of GHGs (including ODSs) alone on the changes in tropospheric O_3 between 1960 and present-day. However, *Shindell et al.* [2006] examined the difference in O_3 between preindustrial and present-day simulations that have differing GHGs and precursor emissions. Their Figure 13b shows results that are qualitatively similar to those shown in Figure 4a, i.e., an increase in tropical and NH troposphere and decrease in SH extratropical troposphere and throughout the stratosphere. The increase in NH tropospheric O_3 is much

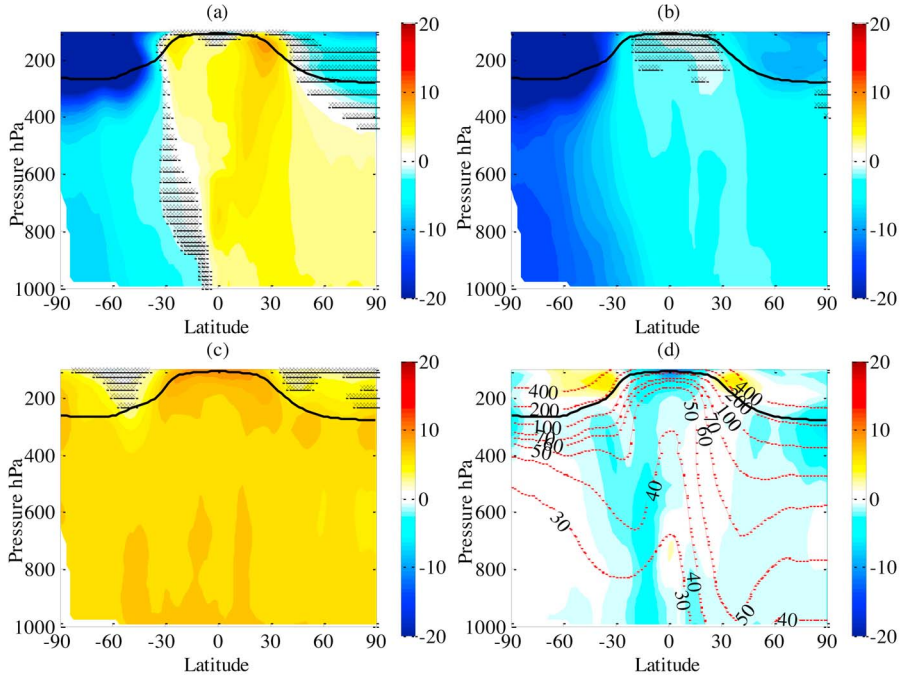

Figure 4. Zonal mean percentage change in O_3 (relative to TS2005) for (a) ΔPast, (b) ΔODS, (c) ΔCH_4 and (d) ΔCO_2. Crosses show regions where the difference is not statistically significant at the 95% confidence level. The tropopause in TS2005 is shown by black thick curve, and the TS2005 climatological O_3 (ppbv) is shown by red contours in Figure 4d.

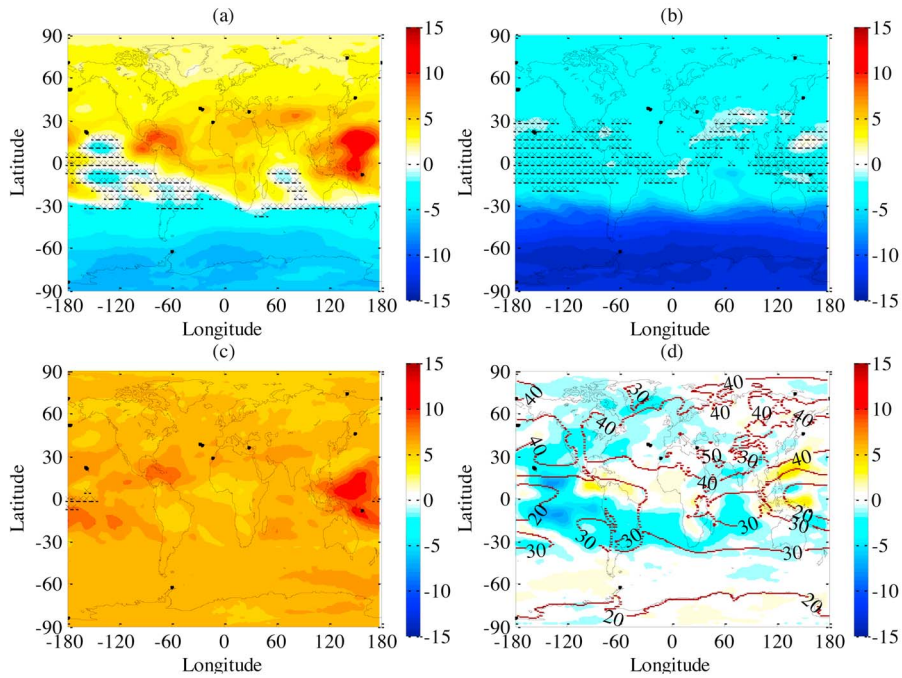

Figure 5. As in Figure 4, except maps showing percentage change in TCO.

larger in *Shindell et al.* [2006] (peak increases of 30%), but this is expected given the increase in precursor emissions and longer time period in their study. The decreases in SH troposphere are also larger in *Shindell et al.* [2006], which appear related to unrealistically large changes in stratospheric O_3 in their simulations (90% decrease in annual-mean O_3 in the Antarctic lower stratosphere and 40% decrease in Arctic lower stratosphere).

[26] The sign of the change in O_3 is generally the same for all seasons, but there are seasonal variations in the magnitude of the change (see Figure S6 in Text S1). In the stratosphere the largest decreases occur in spring (SON for SH, MAM for NH). For example, the October total column O_3 for 60–90S decreases from 353 DU in 1960 to 217 DU in 2005, consistent with observations [*World Meteorological Organization*, 2011]. There is also large seasonality in the magnitude of the O_3 decrease near the extra-tropical tropopause. For both the SH and NH polar tropopause, the seasonality of O_3 change is not in phase with the change in the stratosphere, with the maximum decrease near the tropopause occurring in summer or fall rather than spring. Throughout most of the troposphere there are only weak seasonal variations in the change in O_3. The exception is southern high latitudes, where the decrease in May–June is around twice that in November–December (see Section 4.2).

[27] To investigate the zonal variations in the change in tropospheric O_3 we examine the percentage changes in annual-mean tropospheric column ozone (TCO) and surface O_3; see Figures 5a and 6a. The latitudinal variations seen in the changes in zonal mean O_3 can also be seen in the TCO, with decreases in SH and increases in the tropics and NH. There are limited longitudinal variations in middle and high latitudes of both hemispheres, but there are longitudinal variations in the tropics and subtropics, with increases (>8%) over the western tropical Pacific and northern tropical Atlantic, and statistically insignificant decreases over the central-eastern Pacific and southern Indian Ocean. The regions with largest percentage increases in TCO are also the regions with lowest climatological values (see Figure 3), and there are much smaller longitudinal variations in the absolute change in TCO.

[28] The general features of the change in surface O_3 are similar to that in TCO (see Figure 6a): Surface O_3 decreases in SH high latitudes, increases in the tropics and NH, and the largest longitudinal variations occur in the tropics. The magnitude of the percentage change of surface O_3 is also similar to that of TCO. The amplitude of the longitudinal variance in tropical surface O_3 is, however, larger than that of TCO. Also, there are longitudinal variations at middle latitude surface O_3 not found in TCO.

[29] It would be interesting to evaluate the reality of the simulated 1960 to 2005 changes in tropospheric O_3. However, the impacts of increases in emissions of ozone precursor gases (e.g., NO_x) are not included in the simulations, and these increases are likely a major factor in observed changes in tropospheric O_3. Although a sensible comparison could be possible in the SH where smaller anthropogenic emissions of precursor gases, there are insufficient long-term measurements in the SH that can be used to assess the simulated tropospheric O_3 change between the 1960s and 2000s (e.g., the longest surface record is from the South Pole station, and measurements there are only from 1975).

[30] The changes described above are due to changes in several GHGs. As described in section 2, we isolate the role of the different GHGs by calculating the difference between the TS2005 simulation and the additional "2005" simulations, i.e., ΔODS and ΔCH_4. We next discuss the impacts of increases in ODSs on the simulated O_3, and then discuss the impact of CH_4, and finally the combined impact of CO_2, N_2O, and SSTs.

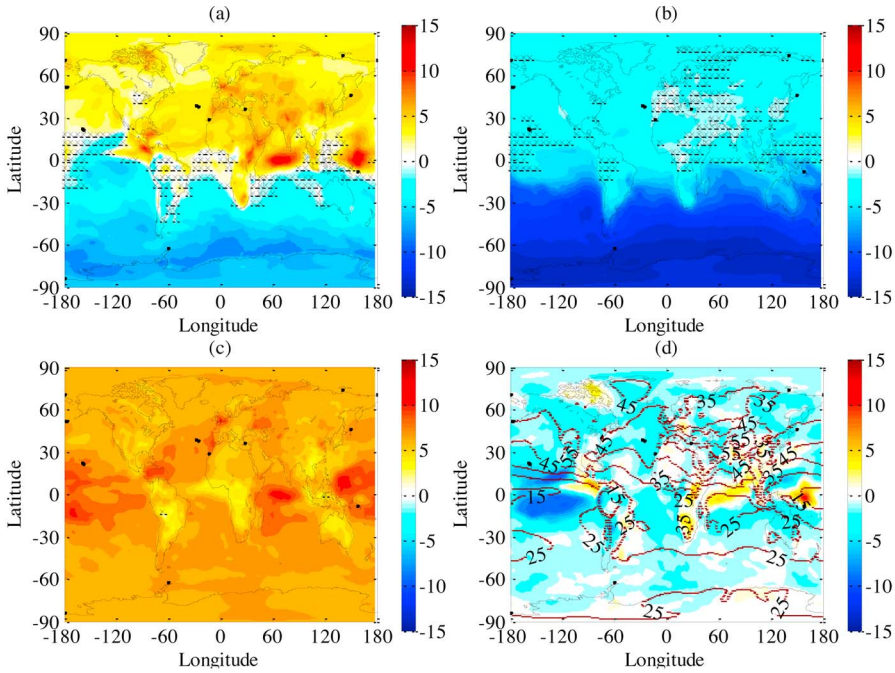

Figure 6. As in Figure 4, except maps showing percentage change in surface O_3.

4.2. Impact of ODSs

[31] The increases in ODSs from 1960 to 2005 cause a decrease in O_3 throughout the troposphere and stratosphere in both hemispheres; see Figure 4b. The largest decrease occurs in the SH extratropics, with similar magnitude decreases of 10–20% occurring from the surface to mid-troposphere and much larger decreases in the upper troposphere and stratosphere. In the NH and tropics the decreases of tropospheric O_3 are much smaller (1–5%).

[32] Comparison of Figures 4a and 4b shows that the increase in ODSs explains the large decreases in stratospheric O_3, i.e., the change due to all GHGs is similar to that due just to ODSs. This also holds for changes for each month, and the seasonality of the change in stratospheric ozone due to ODSs is the same as that for all GHGs.

[33] This is not the case in the troposphere and around the tropopause, where the change in O_3 due to all GHGs is of smaller magnitude or even a different sign than the change due to ODSs. Thus, changes in the other GHGs play an important role in changes in tropospheric O_3, and these changes are discussed in section 4.3.

[34] The ODS-induced changes in tropospheric O_3 are due primarily to changes in stratospheric O_3 rather than changes in tropospheric climate caused by the greenhouse gas effect of ODS change. There are two primary mechanisms by which reductions in stratospheric O_3 caused by increasing ODSs can then alter tropospheric O_3: (i) stratospheric O_3 depletion reduces the transport of O_3 from the stratosphere into troposphere and (ii) stratospheric O_3 depletion lets more UV penetrate into troposphere which will change O_3 concentration (via change photolysis reactions) [*Fuglestvedt et al.*, 1994; *Karlsdòttir et al.*, 2000; *Lelieveld and Dentener*, 2000; *Thompson*, 1991]. The calculations of *Karlsdòttir et al.* [2000] suggest that STE contributed 60% of the 1980 to 1996 tropospheric O_3 change caused by stratospheric O_3 depletion.

[35] Although we cannot determine the relative role of STE and UV in this study, some insight into the role of the different mechanisms can be gained by examination of the seasonal variation in the O_3 trends at different levels. Figure 7a shows the seasonal variation in the change in southern high latitude O_3 due to the past increase in ODSs (ΔODS). The maximum decrease in O_3 mixing ratio at 100 hPa occurs in October but is shifted to December for 250 hPa, and to May for 500 hPa. This delay in the peak decrease is consistent with the transport of air from the stratosphere into the middle and lower troposphere, indicating a major role due to STE. However, Figure 7a also shows a $\sim$10% decrease in tropospheric O_3 at the same time as there is peak stratospheric O_3 depletion. Coincident with this there is an increase in SH high latitude tropospheric OH (Figure 7b). This indicates that stratospheric O_3 depletion induced changes in UV (which therefore causes OH increases) is also playing a role in the change in tropospheric O_3.

[36] The change in simulated O_3 STE can be calculated using the mass balance approach described in section 3. Table 3 lists the change in mass and O_3 STE between simulations. For ΔODS there is a significant decrease in O_3 STE in both hemispheres: -15.3 and -45.4 Tg/y in NH and SH, respectively, which corresponds to decreases of 5.4% and 21.6%. The cause of the change in O_3 STE is the ODS-induced decrease in stratospheric O_3. However, increases in ODS also change the stratospheric circulation and the mass flux into the troposphere [e.g., *Oman et al.*, 2009], and for ΔODS there is a small increase in the mass STE (1.4% for NH and 0.9% for SH). This increased mass STE results in a small offset of the effect of stratospheric O_3 depletion on O_3 STE.

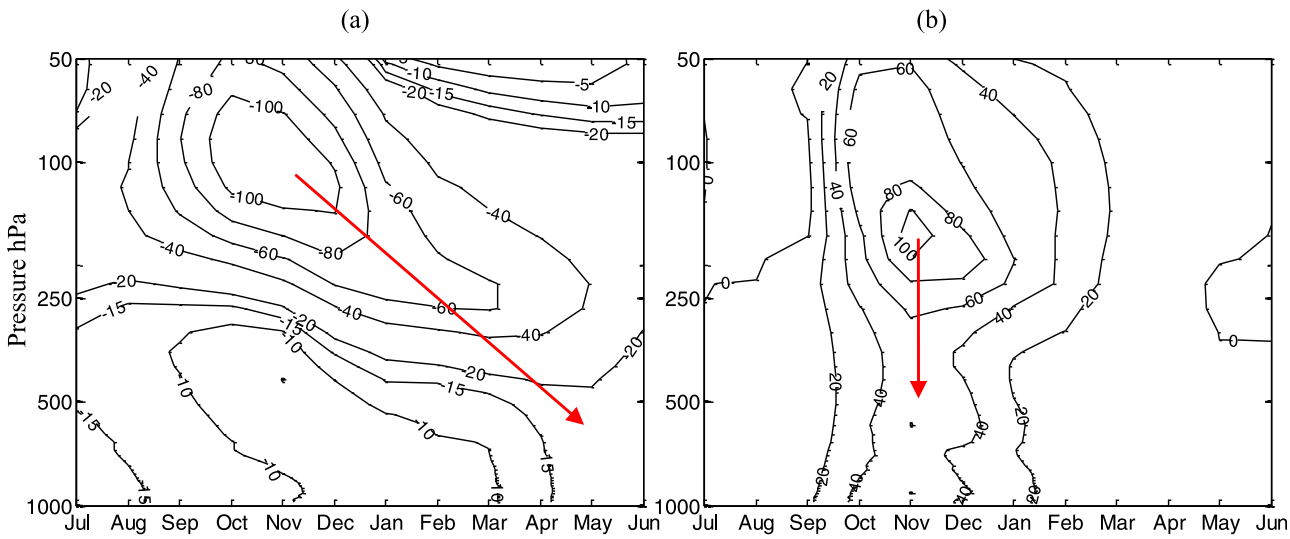

Figure 7. Altitude-seasonal change in percentage change in 60–90S mean mixing ratio of (a) O_3 and (b) OH for ΔODS. Red arrows indicate the month of maximum change at each level.

4.3. Impact of CH_4

[37] We now consider the impact of the 1960 to 2005 increases in CH_4 on O_3 (i.e., ΔCH_4). In contrast to the decrease for ΔODS, there is an increase in O_3 throughout the troposphere for ΔCH_4 (Figure 4c). The percentage increase is fairly constant through the troposphere (around 6%), except near the surface and in the tropical upper troposphere where there are larger increases (~8%). The seasonal variation of O_3 change due to CH_4 is very weak except near tropical tropopause where O_3 has maximum increase in July. In the NH and tropical troposphere, the magnitude of the increase in O_3 due to CH_4 is larger than the decrease due to ΔODS, and the combined effect of increased CH_4 and ODSs is an increase in O_3. The reverse occurs in SH extratropics, and the combined effect is a decrease in O_3.

[38] As discussed in the Introduction, O_3 could be generated through the CH_4 oxidation in the presence of NO_x, and many previous modeling studies have shown an increase in O_3 from increased CH_4 emissions [*Fiore et al.*, 2008, and references therein]. *Fiore et al.* [2008] have shown that the change in tropospheric O_3 burden is nearly linearly correlated with the change in CH_4 emissions (see their Figure 1). To compare our results with this relationship, we estimate the change in CH_4 emissions in our simulations by assuming CH_4 is in steady state with a balance between emission and loss via the CH_4-OH reaction. At each grid point the CH_4 loss is calculated from the CH_4 and OH mixing ratios, and these losses are then summed over the troposphere to yield the effective emissions. This calculation yields an increase of 100 Tg/yr for CH_4 emissions for ΔCH_4. (This is likely an overestimate of the real increase in emissions as the model OH is calculated with 2005 abundances of other ozone precursors and water vapor, which are most likely higher than the 1960 values.) Combining this estimate with the simulated increase in tropospheric O_3 burden of 23 Tg implies an increase in burden of 0.23 Tg for each additional Tg/year of CH_4 emission. This sensitivity of O_3 burden to CH_4 emissions is within the spread for simulations shown in Figure 1 of *Fiore et al.* [2008], although larger than most simulations.

[39] One possibility for a higher sensitivity could be a bias in our simple estimation of the change in CH_4 emissions.

Table 3. O_3 STE Flux, Mass STE Flux and Lowermost Stratospheric O_3 Mixing Ratio for TS2005 Climatology and for Differences Between Simulations[a]

		O_3 STE Flux (Tg/y)	Mass STE Flux (10^6 Tg/y)	Lowermost Stratosphere O_3 Mixing Ratio (ppb)
North Hemisphere	TS2005	284.9 (16.5)	262.3 (8.9)	656.3 (28.1)
	ΔPast	6.4	16.7	−29.0
	ΔODS	−15.3	3.6	−45.0
	ΔCH_4	14.7	4.9	22.0
	ΔCO_2	7.1	8.2	−6.0
South Hemisphere	TS2005	210.3 (10.2)	233.1 (8.4)	545.1 (19.4)
	ΔPast	−26.1	13.6	−106.0
	ΔODS	−45.4	2.2	−123.9
	ΔCH_4	5.4	1.3	10.5
	ΔCO_2	13.9	10.1	7.4

[a]Numbers in brackets for TS2005 correspond to one interannual standard variation.

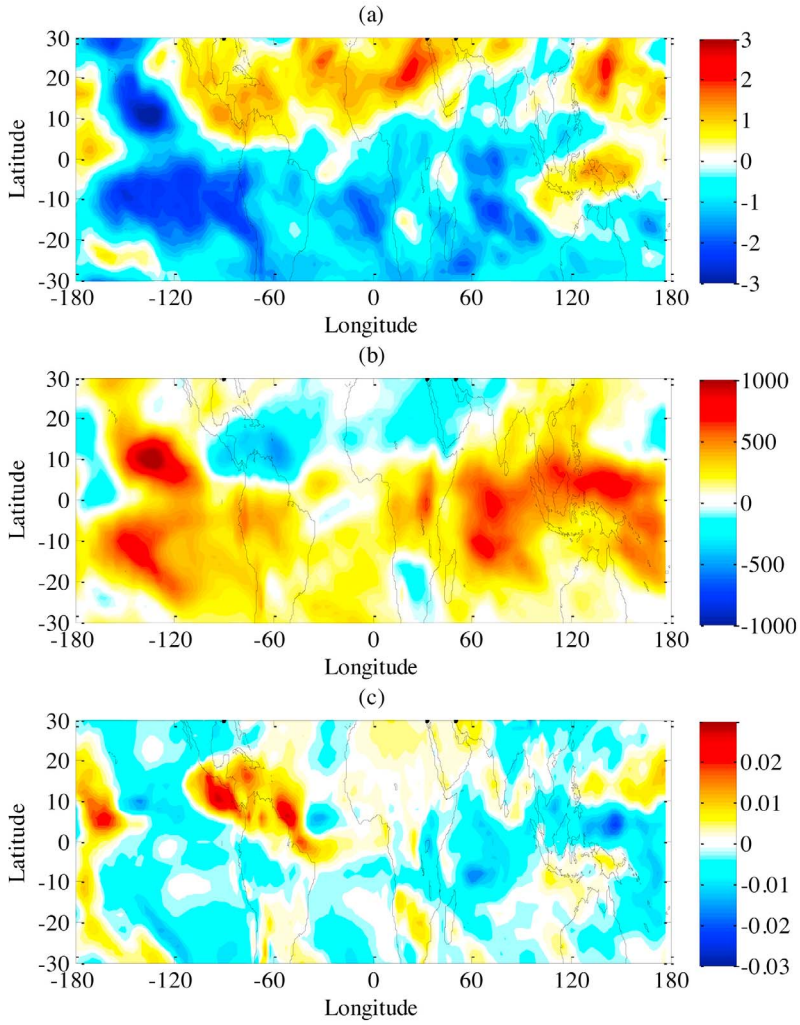

Figure 8. Maps of the change in annual-mean 500 hPa (a) O_3 (ppbv), (b) water vapor (ppmv) and (c) vertical velocity (Pa/S) for ΔCO_2.

Another possible cause of the higher sensitivity of tropospheric O_3 burden to CH_4 emissions in our calculations is the inclusion of couplings between dynamics and chemistry and between the stratosphere and troposphere in GEOS CCM (which are absent from most models considered in *Fiore et al.* [2008]). Figure 4c shows that there is an increase in lower stratospheric O_3 in ΔCH_4 (see *Fleming et al.* [2011] for discussion of mechanism involved). Furthermore, there is an increase in the mass STE in ΔCH_4 (Table 3), which is likely related to a change in meridional temperature gradients in the lower stratosphere (there is 0.4 K increase of temperature in the tropics and 1 K decrease at high latitudes). The combined increases in lower stratospheric O_3 and mass STE result in O_3 STE increases in both hemispheres: 14.7 Tg/y (~5%) for NH and 5.4 Tg/y (~2.5%) for SH (Table 3). These changes will increase tropospheric O_3 burden, and contribute toward a higher sensitivity of tropospheric O_3 burden to CH_4 emissions.

4.4. Impact of CO_2 and SSTs

[40] We finally consider the impact of increases in CO_2 and SSTs on tropospheric O_3, i.e., the change for ΔCO_2. As described in section 2, this is calculated as the residual ΔPast − ΔODS − ΔCH_4 and includes not only the impact of CO_2, N_2O and SSTs but also includes any nonlinearity in the system. (However, as discussed in section 2, climatological monthly mean emissions of NO_x from lightning are used in all simulations, and climate change has no impact on these NO_x emissions in the simulations.) The change in O_3 for ΔCO_2 is much smaller than changes for ΔODSs or ΔCH_4, except in the tropics where there are decreases in zonal mean O_3 of around 5% (Figure 4d). There are large longitudinal variations in the change in tropical O_3 for ΔCO_2, and the decrease in zonal mean tropical O_3 is the balance between regional decreases over the eastern Pacific, southern Atlantic, and Indian Oceans, and increases over the Caribbean and western Pacific (Figures 5d and 6d). The variations for ΔCO_2 are a major cause of longitudinal variations in the total past change of tropical O_3 (compare Figures 5d and 6d with Figures 5a and 6a).

[41] The spatial variations of changes in O_3 are related to similar variations in water vapor and transport. This is shown in Figure 8, which shows the change in 500 hPa O_3, water vapor, and vertical velocity for ΔCO_2. The changes in O_3 are

Table 4. Tropospheric O_3 Burden (in Tg) for Different Regions for the TS2005 Simulation and Differences Between Simulations

	NH Extratropics 90N–30N	NH Tropics 30N-EQ	SH Tropics EQ-30S	SH Extratropics 30S–90S	Global
TS2005	115.7	83.0	72.3	71.1	342.1
ΔPast	4.6	4.7	2.0	−2.5	8.8
ΔODS	−2.7	−1.3	−2.1	−7.2	−13.4
ΔCH_4	7.3	5.8	5.0	4.7	22.8
ΔCO_2	0.0	0.2	−0.8	0.1	−0.6

generally anti-correlated with changes in water vapor, consistent with previous studies reporting more water vapor leading to more O_3 destruction through its photolysis and the subsequent reaction of $O(^1D)$ with water vapor [e.g., *Stevenson et al.*, 2006; *Zeng and Pyle*, 2003; *Zeng et al.*, 2010]. However, this chemical mechanism does not fully explain the spatial variations in composition, and other factors play a role.

[42] One such factor is changes in the circulation (and resulting transport). There is an increase in the upward motion (or weaker downward motion) over the tropical western Pacific, subtropical eastern Pacific, and Indian Oceans (Figure 8c), and in these regions there is a decrease in O_3 and increase in water vapor (Figures 8a and 8b). The reverse (weaker upward or stronger downward, increase in O_3, and decrease in water vapor) occurs over the Caribbean and northern subtropical western Pacific. This connection between O_3 and circulation changes is a combination of direct transport changes and changes in the chemistry. Increased upward transport generally brings lower concentrations O_3 air into the middle-upper troposphere, but also increases water vapor concentration that in turn lead to more O_3 destruction, with the reverse for regions with reduced upward transport (or increased downward transport). Similar coherent variations in tropical circulation – H_2O – O_3 are found with El Niño-Southern Oscillation (ENSO) [e.g., *Sudo and Takahashi*, 2001].

[43] As discussed above, increases in CO_2/SSTs have a relatively small impact outside the tropics. However, there is a notable increase in O_3 STE for ΔCO_2 (Table 3) that should produce an increase in tropospheric burden. The lack of such a change in burden (Table 4) could be because there is opposing increased O_3 destruction due to higher humidity (resulting from increased temperatures).

4.5. Tropospheric Ozone Burden

[44] The relative role the different GHGs play in changing tropospheric O_3 can be quantified by comparing the changes in tropospheric O_3 burden between simulations. The burden changes in tropics (latitude lower than 30°) and extratropics (30° to pole) are calculated separately, see Table 4. As discussed above, the extratropical O_3 changes for ΔPast are dominated by ODSs and CH_4. In the NH extratropics there is a 4.6 Tg increase for ΔPast, which is the difference between a 7.3 Tg increase due to CH_4 and 2.7 Tg decrease due to ODSs. In the SH extratropics the 2.5 Tg decrease in ΔPast is the difference between a 7.2 Tg decrease due to ODSs and 4.6 Tg increase due to CH_4 (with small ΔCO_2 term of 0.1). In the tropics, the change due to CO_2/SST plays a role, but it is still smaller than changes due to CH_4 or ODSs, i.e., ΔCO_2 contributes −0.8 Tg burden change in SH tropics while the total change in the past is 2.0 Tg.

5. Conclusions

[45] The impact of changes in the abundance of greenhouse gases (GHGs) on the evolution of tropospheric O_3 is examined using a version of the Goddard Earth Observing System chemistry-climate model (GEOS CCM) that includes a combined troposphere-stratospheric chemical mechanism. A series of time-slice integrations were performed in which the emissions of non-methane O_3 precursor gases and aerosol distribution are fixed at current day values but the prescribed surface values of GHGs, including methane (CH_4) and stratospheric ozone-depleting substances (ODSs), and SSTs differ between 1960 and 2005 values.

[46] The GEOS CCM simulations indicate that the sign of the change in tropospheric O_3 due to increases in GHGs differs between southern and northern extratropics, with a decrease in the southern extratropics but increases in the northern extratropics and tropics. These O_3 changes are due primarily to increases in CH_4 and ODSs, with changes in the other GHGs (CO_2 and N_2O) and SSTs having only a small impact on the change in tropospheric O_3 burden. Increases in CH_4 lead to in situ production and increases in tropospheric O_3 at all latitudes, whereas increases in ODS leads to decreases in tropospheric O_3. CH_4-related increases dominate in the NH whereas the ODS-related decreases dominate in the SH, resulting in the hemispheric difference in the sign of O_3 trends.

[47] While increases in the other GHGs and SSTs have only a small impact on the total burden, they cause significant zonal variations within the tropics that are coupled to changes in upwelling and humidity. There is reduced O_3 in regions with more upwelling and higher humidity, and increased O_3 in regions with more descending and drier air.

[48] The results from the GEOS CCM simulations indicate that increases in ODS (and resulting stratospheric O_3 depletion) have played an important role in changes of tropospheric O_3 over the past four or five decades, and need to be carefully considered when examining changes over this period. The largest impact is in the SH where there has been the largest stratospheric O_3 depletion, but there is still a significant impact in the global tropospheric burden change from 1960 to 2005, with decreases due to ODS offsetting around half the increase in burden due to CH_4. It is expected that changes in ODS will also be important for coming decades. The concentrations of ODSs are expected to decrease because of the Montreal Protocol and amendments, so the impact of ODS change will be to increase tropospheric O_3 in the future.

[49] Integrations of GEOS CCM for projected changes in ODSs and other GHGs are currently being performed and will be analyzed in a future study. Integrations with differing O_3 precursor emissions are also being performed, and will be used to compare the changes in tropospheric O_3 due to GHGs with corresponding changes in non-methane O_3 precursor emissions that have occurred at the same time.

[50] **Acknowledgments.** This research was supported by the NASA MAP and ACMAP programs. We would like to thank Stacey Frith for helping with the model output processing. We also thank those involved in model development at GSFC, and high-performance computing resources provided by NASA's Advanced Supercomputing Division.

References

Appenzeller, C., J. R. Holton, and K. H. Rosenlof (1996), Seasonal variation of mass transport across the tropopause, *J. Geophys. Res.*, *101*, 15,071–15,078, doi:10.1029/96JD00821.

Bey, I., D. J. Jacob, R. M. Yantosca, J. A. Logan, B. D. Field, A. M. Fiore, Q. B. Li, H. G. Y. Liu, L. J. Mickley, and M. G. Schultz (2001), Global modeling of tropospheric chemistry with assimilated meteorology: Model description and evaluation, *J. Geophys. Res.*, *106*, 23,073–23,095, doi:10.1029/2001JD000807.

Considine, D. B., J. A. Logan, and M. A. Olsen (2008), Evaluation of near-tropopause ozone distributions in the Global Modeling Initiative combined stratosphere/troposphere model with ozonesonde data, *Atmos. Chem. Phys.*, *8*, 2365–2385, doi:10.5194/acp-8-2365-2008.

Douglass, A. R., R. S. Stolarski, S. E. Strahan, and P. S. Connell (2004), Radicals and reservoirs in the GMI chemistry and transport model: Comparison to measurements, *J. Geophys. Res.*, *109*, D16302, doi:10.1029/2004JD004632.

Duncan, B. N., S. E. Strahan, Y. Yoshida, S. D. Steenrod, and N. Livesey (2007), Model study of the cross-tropopause transport of biomass burning pollution, *Atmos. Chem. Phys.*, *7*, 3713–3736, doi:10.5194/acp-7-3713-2007.

Emmons, L. K., D. A. Hauglustaine, J. F. Muller, M. A. Carroll, G. P. Brasseur, D. Brunner, J. Staehelin, V. Thouret, and A. Marenco (2000), Data composites of airborne observations of tropospheric ozone and its precursors, *J. Geophys. Res.*, *105*, 20,497–20,538, doi:10.1029/2000JD900232.

Eyring, V., T. G. Shepherd, and D. W. Waugh (Eds.) (2010), *Chemistry-Climate Model Validation, SPARC Rep. 5, WCRP-30, WMO/TD-40*, SPARC CCMVAL Group, World Clim. Res. Programme, Geneva.

Fiore, A. M., D. J. Jacob, B. D. Field, D. G. Streets, S. D. Fernandes, and C. Jang (2002), Linking ozone pollution and climate change: The case for controlling methane, *Geophys. Res. Lett.*, *29*(19), 1919, doi:10.1029/2002GL015601.

Fiore, A. M., J. J. West, L. W. Horowitz, V. Naik, and M. D. Schwarzkopf (2008), Characterizing the tropospheric ozone response to methane emission controls and the benefits to climate and air quality, *J. Geophys. Res.*, *113*, D08307, doi:10.1029/2007JD009162.

Fleming, E. L., C. H. Jackman, R. S. Stolarski, and A. R. Douglass (2011), A model study of the impact of source gas changes on the stratosphere for 1850–2100, *Atmos. Chem. Phys.*, *11*, 8515–8541, doi:10.5194/acp-11-8515-2011.

Fuglestvedt, J. S., J. E. Jonson, and I. S. A. Isaksen (1994), Effects of reductions in stratospheric ozone on tropospheric chemistry through changes in photolysis rates, *Tellus, Ser. B*, *46*, 172–192, doi:10.1034/j.1600-0889.1992.t01-3-00001.x-i1.

Gauss, M., et al. (2006), Radiative forcing since preindustrial times due to ozone change in the troposphere and the lower stratosphere, *Atmos. Chem. Phys.*, *6*, 575–599, doi:10.5194/acp-6-575-2006.

Hegglin, M. I., and T. G. Shepherd (2009), Large climate-induced changes in ultraviolet index and stratosphere-to-troposphere ozone flux, *Nat. Geosci.*, *2*, 687–691, doi:10.1038/ngeo604.

Intergovernmental Panel on Climate Change (2007), *Climate Change 2007: The Physical Science Basis. Contribution of Working Group I to the Fourth Assessment Report of the Intergovernmental Panel on Climate Change*, edited by S. Solomon et al., Cambridge Univ. Press, Cambridge, U. K.

Karlsdòttir, S., I. S. A. Isaksen, and G. Myhre (2000), Trend analysis of O_3 and CO in the period 1980–1996: A three-dimensional model study, *J. Geophys. Res.*, *105*, 28,907–28,933.

Lamarque, J. F., and S. Solomon (2010), Impact of changes in climate and halocarbons on recent lower stratosphere ozone and temperature trends, *J. Clim.*, *23*, 2599–2611, doi:10.1175/2010JCLI3179.1.

Lamarque, J. F., et al. (2010), Historical (1850–2000) gridded anthropogenic and biomass burning emissions of reactive gases and aerosols: Methodology and application, *Atmos. Chem. Phys.*, *10*, 7017–7039, doi:10.5194/acp-10-7017-2010.

Lelieveld, J., and F. J. Dentener (2000), What controls tropospheric ozone? *J. Geophys. Res.*, *105*, 3531–3551, doi:10.1029/1999JD901011.

Li, F., R. S. Stolarski, and P. A. Newman (2009), Stratospheric ozone in the post-CFC era, *Atmos. Chem. Phys.*, *9*, 2207–2213, doi:10.5194/acp-9-2207-2009.

Liang, Q., A. R. Douglass, B. N. Duncan, R. S. Stolarski, and J. C. Witte (2009), The governing processes and timescales of stratosphere-to-troposphere transport and its contribution to ozone in the Arctic troposphere, *Atmos. Chem. Phys.*, *9*, 3011–3025, doi:10.5194/acp-9-3011-2009.

Logan, J. A. (1999), An analysis of ozonesonde data for the troposphere: Recommendations for testing 3-D models and development of a gridded climatology for tropospheric ozone, *J. Geophys. Res.*, *104*, 16,115–16,149, doi:10.1029/1998JD100096.

Newman, P. A., et al. (2009), What would have happened to the ozone layer if chlorofluorocarbons (CFCs) had not been regulated?, *Atmos. Chem. Phys.*, *9*, 2113–2128, doi:10.5194/acp-9-2113-2009.

Novelli, P. C., and K. A. Masarie (2010), *Atmospheric Carbon Monoxide Dry Air Mole Fractions from the NOAA ESRL Carbon Cycle Cooperative Global Air Sampling Network, 1988–2009, Version: 2010-07-14*, Global Monit. Div., NOAA Earth Syst. Res. Lab., Boulder, Colo.

Olsen, M. A., M. R. Schoeberl, and A. R. Douglass (2004), Stratosphere-troposphere exchange of mass and ozone, *J. Geophys. Res.*, *109*, D24114, doi:10.1029/2004JD005186.

Olsen, M., A. R. Douglass, and T. Kaplan (2012), Variability of extratropical ozone stratosphere-troposphere exchange using Microwave Limb Sounder observations, *J. Geophys. Res.*, doi:10.1029/2012JD018465, in press.

Oman, L., D. W. Waugh, S. Pawson, R. S. Stolarski, and P. A. Newman (2009), On the influence of anthropogenic forcings on changes in the stratospheric mean age, *J. Geophys. Res.*, *114*, D03105, doi:10.1029/2008JD010378.

Oman, L., J. R. Ziemke, A. R. Douglass, D. W. Waugh, C. Lang, J. M. Rodriguez, and J. E. Nielsen (2011), The response of tropical tropospheric ozone to ENSO, *Geophys. Res. Lett.*, *38*, L13706, doi:10.1029/2011GL047865.

Pawson, S., R. S. Stolarski, A. R. Douglass, P. A. Newman, J. E. Nielsen, S. M. Frith, and M. L. Gupta (2008), Goddard Earth Observing System chemistry-climate model simulations of stratospheric ozone-temperature coupling between 1950 and 2005, *J. Geophys. Res.*, *113*, D12103, doi:10.1029/2007JD009511.

Rayner, N. A., D. E. Parker, E. B. Horton, C. K. Folland, L. V. Alexander, D. P. Rowell, E. C. Kent, and A. Kaplan (2003), Global analyses of sea surface temperature, sea ice, and night marine air temperature since the late nineteenth century, *J. Geophys. Res.*, *108*(D14), 4407, doi:10.1029/2002JD002670.

Rienecker, M. M., et al. (2008), *The GEOS-5 Data Assimilation System-Documentation of Versions 5.0.1, 5.1.0, and 5.2.0 Technical Report Series on Global Modeling and Data Assimilation*, vol. 27, NASA GSFC, Greenbelt, Md.

Shindell, D. T., G. Faluvegi, N. Unger, E. Aguilar, G. A. Schmidt, D. M. Koch, S. E. Bauer, and R. L. Miller (2006), Simulations of preindustrial, present-day, and 2100 conditions in the NASA GISS composition and climate model G-PUCCINI, *Atmos. Chem. Phys.*, *6*, 4427–4459, doi:10.5194/acp-6-4427-2006.

Shindell, D. T., G. Faluvegi, D. M. Koch, G. A. Schmidt, N. Unger, and S. E. Bauer (2009), Improved attribution of climate forcing to emissions, *Science*, *326*, 716–718, doi:10.1126/science.1174760.

Stevenson, D. S., et al. (2006), Multimodel ensemble simulations of present-day and near-future tropospheric ozone, *J. Geophys. Res.*, *111*, D08301, doi:10.1029/2005JD006338.

Stolarski, R. S., A. R. Douglass, P. A. Newman, S. Pawson, and M. R. Schoeberl (2010), Relative contribution of greenhouse gases and ozone-depleting substances to temperature trends in the stratosphere: A chemistry-climate model study, *J. Clim.*, *23*, 28–42, doi:10.1175/2009JCLI2955.1.

Strahan, S. E., B. N. Duncan, and P. Hoor (2007), Observationally derived transport diagnostics for the lowermost stratosphere and their application to the GMI chemistry and transport model, *Atmos. Chem. Phys.*, *7*, 2435–2445, doi:10.5194/acp-7-2435-2007.

Sudo, K., and M. Takahashi (2001), Simulation of tropospheric ozone changes during 1997–1998 El Nino: Meteorological impact on tropospheric photochemistry, *Geophys. Res. Lett.*, *28*, 4091–4094, doi:10.1029/2001GL013335.

Sudo, K., M. Takahashi, and H. Akimoto (2003), Future changes in stratosphere-troposphere exchange and their impacts on future tropospheric ozone simulations, *Geophys. Res. Lett.*, *30*(24), 2256, doi:10.1029/2003GL018526.

Thompson, A. M. (1991), New ozone hole phenomenon, *Nature*, *352*, 282–283, doi:10.1038/352282a0.

Wang, Y. H., and D. J. Jacob (1998), Anthropogenic forcing on tropospheric ozone and OH since preindustrial times, *J. Geophys. Res.*, *103*, 31,123–31,135, doi:10.1029/1998JD100004.

Waugh, D. W., L. Oman, S. R. Kawa, R. S. Stolarski, S. Pawson, A. R. Douglass, P. A. Newman, and J. E. Nielsen (2009), Impacts of climate change on stratospheric ozone recovery, *Geophys. Res. Lett.*, *36*, L03805, doi:10.1029/2008GL036223.

World Health Organizaton (2006), *Air Quality Guidelines: Global Update 2005. Particulate Matter, Ozone, Nitrogen Dioxide and Sulfur Dioxide*, Book News, Inc., Portland, Ore.

World Meteorological Organization (2011), Scientific assessment of ozone depletion: 2010, *Rep. 52*, 438 pp., Global Ozone Res. and Monit. Proj., World Meteorol. Org., Geneva.

Wu, S., L. J. Mickley, D. J. Jacob, D. Rind, and D. G. Streets (2008), Effects of 2000–2050 changes in climate and emissions on global tropospheric ozone and the policy-relevant background surface ozone in the United States, *J. Geophys. Res.*, *113*, D18312, doi:10.1029/2007JD009639.

Zeng, G., and J. A. Pyle (2003), Changes in tropospheric ozone between 2000 and 2100 modeled in a chemistry-climate model, *Geophys. Res. Lett.*, *30*(7), 1392, doi:10.1029/2002GL016708.

Zeng, G., J. A. Pyle, and P. J. Young (2008), Impact of climate change on tropospheric ozone and its global budgets, *Atmos. Chem. Phys.*, *8*, 369–387, doi:10.5194/acp-8-369-2008.

Zeng, G., O. Morgenstern, P. Braesicke, and J. A. Pyle (2010), Impact of stratospheric ozone recovery on tropospheric ozone and its budget, *Geophys. Res. Lett.*, *37*, L09805, doi:10.1029/2010GL042812.

Ziemke, J. R., S. Chandra, B. N. Duncan, L. Froidevaux, P. K. Bhartia, P. F. Levelt, and J. W. Waters (2006), Tropospheric ozone determined from Aura OMI and MLS: Evaluation of measurements and comparison with the Global Modeling Initiative's Chemical Transport Model, *J. Geophys. Res.*, *111*, D19303, doi:10.1029/2006JD007089.